

Singleelectron transfer in collisions of He²⁺ with NH₃ and H₂S: Vibrational state populations of NH⁺ 3 and H₂S⁺

Michal Fárník, Zdenek Herman, Thomas Ruhaltinger, and J. Peter Toennies

Citation: *The Journal of Chemical Physics* **103**, 3495 (1995); doi: 10.1063/1.470233

View online: <http://dx.doi.org/10.1063/1.470233>

View Table of Contents: <http://scitation.aip.org/content/aip/journal/jcp/103/9?ver=pdfcov>

Published by the [AIP Publishing](#)

Articles you may be interested in

[Nascent vibrational populations in He^{*}\(21,3 S\)+H₂, HD, D₂ Penning ionization from electron spectroscopy in crossed supersonic molecular beams](#)

J. Chem. Phys. **102**, 133 (1995); 10.1063/1.469383

[Semiclassical investigation of vibrational state and molecular orientation effects in electron transfer reactions for the H⁺ 2/H₂ collision](#)

J. Chem. Phys. **80**, 1116 (1984); 10.1063/1.446840

[Energy transfer in NH₃–He collisions](#)

J. Chem. Phys. **73**, 2740 (1980); 10.1063/1.440495

[Double and triple resonance studies of rotational relaxation in NH₃–He and NH₃–H₂ collisions](#)

J. Chem. Phys. **68**, 3897 (1978); 10.1063/1.436198

[Electron transfer and excitation in collisions of He⁺⁺ with H](#)

J. Chem. Phys. **58**, 2043 (1973); 10.1063/1.1679468



Single-electron transfer in collisions of He^{2+} with NH_3 and H_2S : Vibrational state populations of NH_3^+ and H_2S^+

Michal Fárnik,^{a)} Zdenek Herman,^{a)} Thomas Ruhaltinger, and J. Peter Toennies
Max-Planck Institut für Strömungsforschung, Bunsenstrasse 10, D-37073 Göttingen, Germany

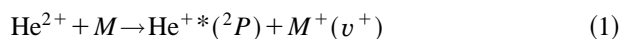
(Received 24 March 1995; accepted 10 May 1995)

Single-electron charge transfer between He^{2+} and NH_3 and H_2S was investigated at the projectile energy of 70 eV by the translational energy spectroscopy method with a resolution of 120 meV. The products were $\text{He}^{+*}(^2P)$ and the ground state molecular ion. Populations of the vibrational states of the molecular ion were derived from the spectra. The vibrational state distributions differ only slightly from the distributions obtained by photoelectron spectroscopy and the differences can be qualitatively accounted for by distortions of the equilibrium configuration of the target molecule by the approaching ion projectile. © 1995 American Institute of Physics.

I. INTRODUCTION

Charge transfer (electron capture) between multiply charged ions and atoms or molecules represents—because of its large cross section—an important class of collision processes. Charge transfer collisions of multiply charged ions have been recently subjected to intensive investigation both at high and low collision energies.^{1,2} Besides atomic ion-atom processes also processes involving molecular species have been investigated in translational energy spectroscopy (TES) studies with the aim of determining both integral and differential cross sections of the respective state-to-state processes. So far, however, there has been little information on the population of vibrational states of the molecular product species. This has been due to a limited energy resolution of the experiments. In addition, the problem may be complicated by dissociative processes, especially in the case of molecular targets. Addressing the problem of product vibrational states population thus requires high-resolution studies and a choice of a suitable simple system in which dissociative processes do not take place.

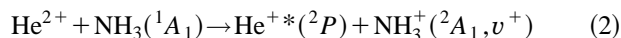
Recently, we have found a class of processes which appear to be suitable for studies of charge transfer between doubly-charged atomic ions and molecular targets. In charge transfer collisions between He^{2+} [IP=79.00 eV (Refs. 3 and 4)] and molecules of an ionization potential of 9–10 eV the reaction window concept may favor the formation of the excited $\text{He}^{+*}(^2P)$ product [IP=65.4 eV (Refs. 3 and 4)] and the ground state molecular ion in which population of vibrational states can be analyzed by high-resolution translational energy spectroscopy (about 3 eV is assumed to go into the relative translational energy of the two positively charged product ions)



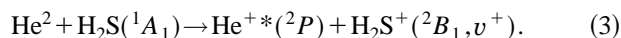
(v^+ refers to a vibrational state of the ion).

Recently, we have applied this method successfully to the investigation of the vibrational state populations of $\text{NO}^+(^1\Sigma^+)$ formed in collisions of 70 eV He^{2+} with NO .⁵

In this communication we report on analogous studies, investigating the population of vibrational states of NH_3^+ and H_2S^+ formed in charge transfer collisions of 70 eV He^{2+} with these molecules

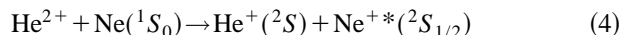


and



Reaction (2) is exoergic by 3.42 eV [IP(NH_3)=10.183 eV (Refs. 6 and 7)], reaction (3) by 3.13 eV [IP(H_2S)=10.466 eV (Ref. 8)], if vibrationally ground state ($v^+=0$) molecular ions are formed. We take again advantage of the doubly charged helium ions as projectiles: simplicity of the projectile devoid of electrons, convenient energetics, and its low mass which even at collision energies of about 100 eV makes the effective collision time shorter than a vibrational period of the target molecule.

In addition, the atomic ion-atom reaction



was investigated to determine not only the final resolution of the machine, but also the peak shape of the He^+ product ion and to calibrate the energy scale. The excited $\text{Ne}^{+*}(^2S_{1/2})$ state of the neon atom [IP=48.48 eV (Refs. 3 and 4)] is formed in reaction (4) which makes it exoergic by 5.93 eV.

II. EXPERIMENT

The Göttingen crossed beam scattering machine (Fig. 1) used earlier in high-resolution proton energy loss spectroscopy studies was adapted for the present experiments. The performance of the machine in energy loss studies of collisions between protons and deuterons and polyatomic molecules (resolution 15–30 meV) was described earlier.⁹

For the purpose of the experiments described here the reactant He^{2+} ions were produced in a Colutron gas-discharge source (Q), extracted (01), mass selected by the Wien filter (WF), focused (02) and energy selected by passing through a tandem hemispherical electrostatic energy analyzer (ES) of mean radii of 4 and 8 cm, respectively. The beam of energy of 70 eV was then focused (03) onto a skimmed nozzle beam (SD) of target beam molecules at right

^{a)}Permanent address: J. Heyrovský Institute of Physical Chemistry, Academy of Sciences of the Czech Republic, Dolejškova 3, 182 23 Prague 8.

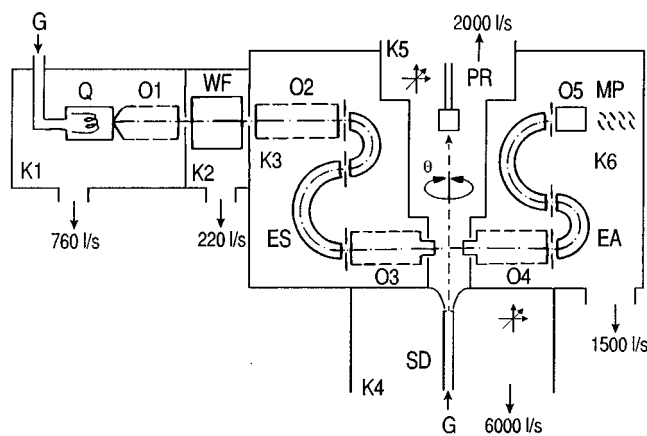


FIG. 1. Schematics of the crossed beam apparatus. Q, Colutron ion source; O1, ion extraction optics; WF, Wien filter; O2..O5, ion focusing optics; ES, energy selector; SD, skimmed nozzle beam; EA, energy analyzer; MP, electron multiplier; G, gas inlets; K1..K6, differentially pumped chamber.

angles. The product ions were then analyzed by a detection system consisting of a focusing lens (O4) and another tandem electrostatic energy analyzer (EA), identical in design with the reactant beam energy selector, followed by a focusing

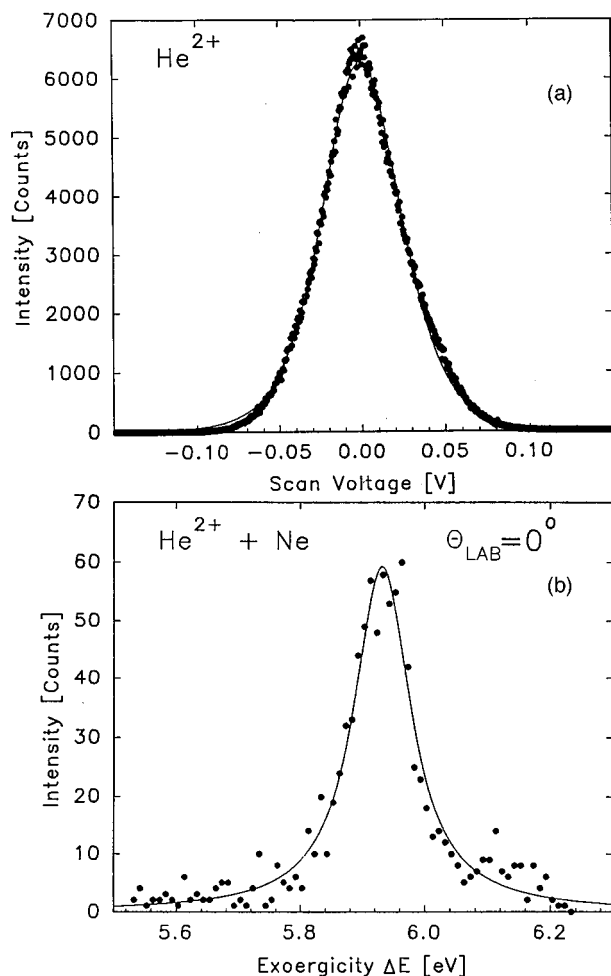


FIG. 2. (a) Energy profile of the ion reactant beam He²⁺. (b) energy profile of the Ne⁺ product from reaction (4) at $\theta=0^\circ$.

lens (O5) and an open venetian blind electron multiplier (MP). The entire analyzer detection system could be rotated about the axis of the target beam in a perpendicular-plane arrangement.

The reactant He²⁺ ions pass through the electrostatic analyzers at 0.5 of their true laboratory energy E ; the energy spectra are then recorded as $0.5E - E + \Delta E'$ translational energy spectra of the He²⁺ reactant and the He⁺ product ($\Delta E'$ is the energy gain from the exoergicity of the process). The intensities of the reactant beam were about 100 cps at the beam energy of 70 eV, and the resolution for doubly-charged ions was about 80 meV [Fig. 2(a)]. The overall resolution of the apparatus was determined by measuring the peak width of the Ne⁺ product from reaction (4). The Gaussian-peak computer fit (Jandel Scientific Peakfit Program, Version 3.00) gave the resolution for product ions of 120 meV, full width at half-maximum (FWHM).

The translational energy spectra of the product ions were recorded at several laboratory scattering angles between 0° and 4° . The translational energy spectra were converted into the reaction exoergicity scale using the kinematic equation¹⁰

$$\Delta E = \left(1 + \frac{m_1}{m_2}\right) E_K - \left(1 - \frac{m_1}{m_2}\right) E_1 - 2 \frac{m_1}{m_2} (E_1 E_K)^{1/2} \cos \theta, \quad (5)$$

where ΔE is the reaction exoergicity, E_1 is the laboratory energy of the projectile He²⁺, E_K is the measured laboratory energy of the He⁺ product, and m_1 and m_2 are the masses of the ion and neutral reactant, respectively. A correction (2.93 eV) was applied to the measured energy E_K to fit the peak center of He⁺ from reaction (4) to the reaction exoergicity, 5.39 eV; this correction remained, within 20 meV, the same during the measurements with NH₃ and H₂S.

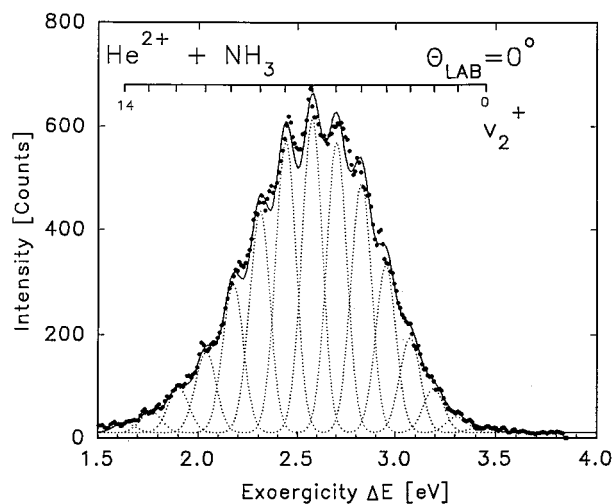


FIG. 3. Translational energy spectrum of He⁺ from reaction with NH₃ at $\theta_{\text{LAB}}=0^\circ$ plotted against the exoergicity of the process, ΔE . Solid line through the measured points is the sum of peaks (dotted) from the computer fit. Resolution 120 meV (FWHM).

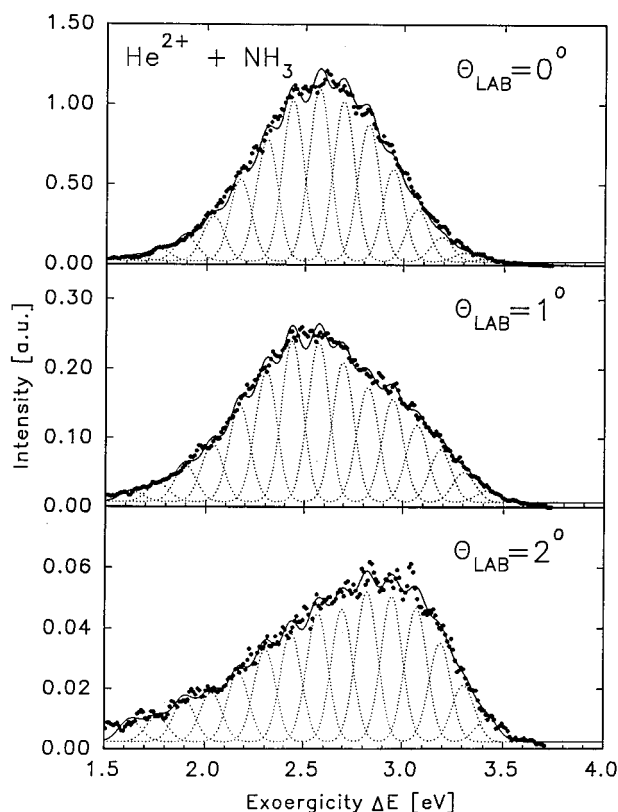


FIG. 4. Translational energy spectra of He⁺ from reaction with NH₃ at the scattering angles 0°, 1°, and 2°; resolution 130 meV. Other details same as in Fig. 3.

III. RESULTS

Figure 3 shows the translational energy spectrum of NH₃⁺ at the laboratory scattering angle $\theta_{\text{LAB}}=0^\circ$. The experimental points show a partly resolved structure of vibrational transitions which correspond well to the exoergicity of reaction (2). The dashed peaks represent a calculated fit using the Gaussian peak shape and the above mentioned resolution of 120 meV. The peaks were placed at the energies of vibrational spacings of the bending mode of NH₃⁺, v_2^+ , as determined from the photoelectron spectra,^{11,12} with $v_2^+=0$ set at the ionization potential IP(NH₃)=10.18 eV. This value results from a thorough theoretical analysis⁶ of the photoelectron spectrum¹¹ and it has been recently confirmed by a ZEKE spectroscopy study.⁷ The peak heights were adjusted to give the best agreement with the experimental points; the solid line is the best fit simulation envelope curve.

Figure 4 shows the laboratory angular dependence of the translational energy spectra of NH₃⁺. The spectra were recorded at the laboratory scattering angles (θ_{LAB}) of 0°, 1°, and 2° at a somewhat lower resolution ($\Delta E=130$ meV) than the spectrum in Fig. 3. The solid line again shows the envelope curve of the best fit with variable heights of the Gaussian peaks. Figure 5 summarizes data on the population of the v_2^+ vibrational levels as derived from the spectra in Figs. 3 and 4. The results are compared with the populations of vibrational levels obtained from the photoelectron spectroscopy data.¹¹ Data in Fig. 5 show that both by photoionization and by charge transfer with He²⁺ a broad band of vibrational

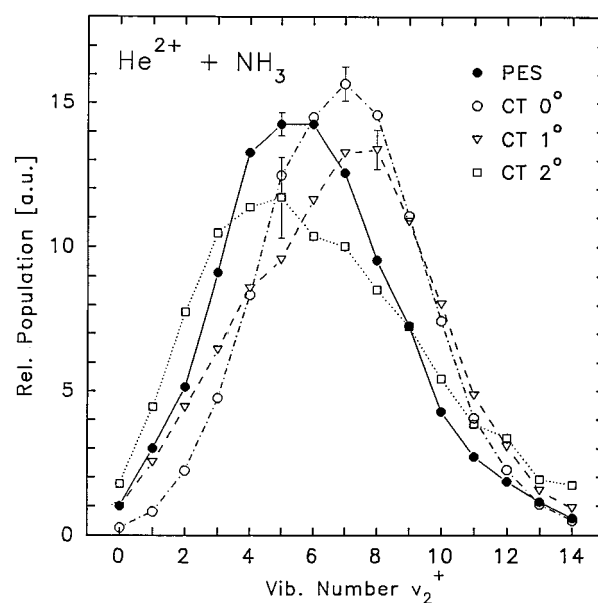


FIG. 5. Relative populations of vibrational levels v_2^+ of the product ion NH₃⁺ from reaction (2) at laboratory scattering angles 0° (○), 1° (▽), and 2° (□); PES (●)—population of vibrational states obtained by photoelectron spectroscopy (Ref. 11). The data are normalized to have the same areas under each of the curves.

states of the NH₃⁺ from $v_2^+=0$ to $v_2^+=14$ is populated. However, the population obtained by charge transfer differs somewhat from that obtained in photoionization and it changes with the scattering angle. The difference is most pronounced at $\theta_{\text{LAB}}=0^\circ$ where the population distribution is shifted with respect to the photoelectron (Franck–Condon) distribution by about two vibrational quanta towards higher levels, peaking at about 7 or 8 and exhibiting a somewhat lower population at low levels and a higher population at high vibrational levels. At the scattering angles 1° and 2° the distribution acquires a shoulder at low v_2^+ which grows with increasing scattering angle. Unfortunately, a sharp decrease of the product ion intensity with the laboratory scattering angle (Fig. 6) prevented reliable measurements of translational energy spectra beyond $\theta_{\text{LAB}}=2^\circ$.

The translational energy spectra from charge transfer collisions of He²⁺ with H₂S at the laboratory scattering angles of 0°, 2°, and 3° are shown in Fig. 7. At $\theta_{\text{LAB}}=0^\circ$ mostly the $v_1^+=0$ vibrational level (symmetric stretch) is populated, with a small shoulder towards lower exoergicities from which a small population of $v_1^+=1$ can be derived. The position of the $v_1^+=0$ peak in the exoergicity scale corresponds well to the IP(H₂S)=10.466 eV obtained by photoelectron spectroscopy⁸ and it agrees, within the limits of accuracy, with a recent more precise value from a ZEKE spectroscopy experiment, 10.469 eV (Ref. 13). With increasing laboratory scattering angles the product ion signal quickly decreases (Fig. 6) and measurements of translational energy spectra beyond 3° were not reliable. Over the region of θ_{LAB} of 0°–3° the low energy shoulder increases and though separate peaks could not be clearly identified, the spectrum analysis (dashed lines in Fig. 7) indicate a slight increase in the population of $v_1^+>0$. The results of this

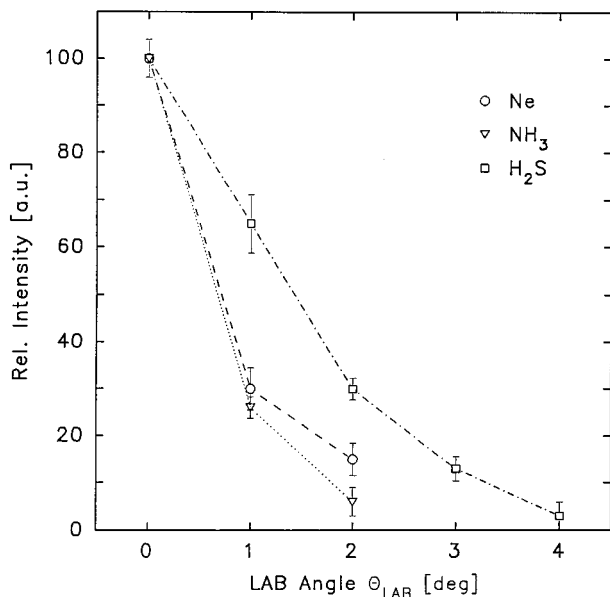


FIG. 6. Comparisons of the total intensities in the translational energy spectra of the He^+ product from reactions with Ne (\circ), NH_3 (∇), and H_2S (\square) at different laboratory scattering angles. The intensities at a particular angle were obtained as sums of all peaks in translational energy spectra and normalized to the intensity at $\theta_{\text{LAB}}=0^\circ$.

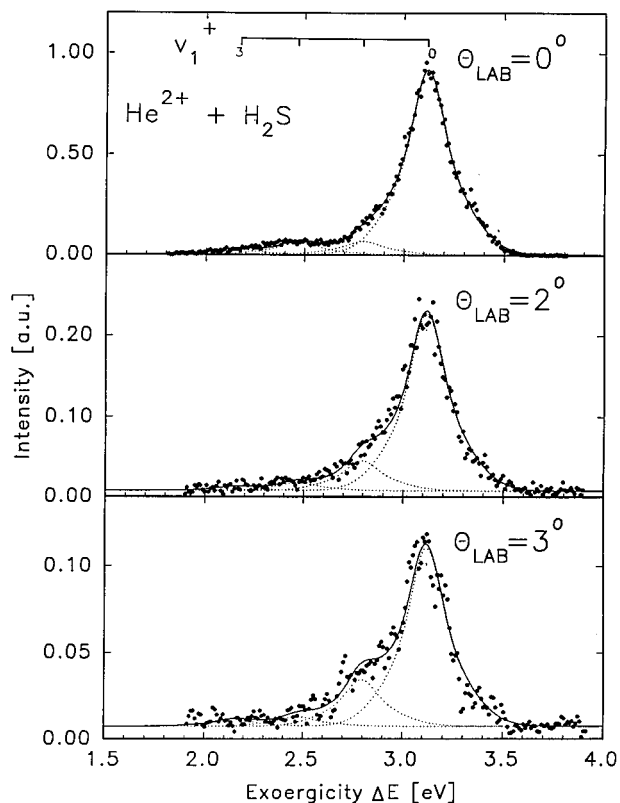


FIG. 7. Translational energy spectra of He^+ from reaction with H_2S at the laboratory scattering angles 0° , 2° , and 3° plotted against the reaction exoergicity ΔE . Solid line through the measured points is the sum of peaks (dotted) resulting from computer fit.

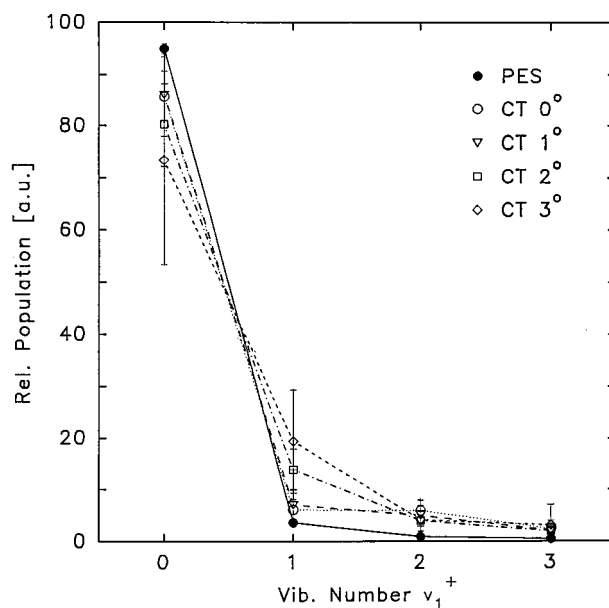


FIG. 8. Relative populations of vibrational levels of the product ion H_2S^+ from reaction (3) at laboratory scattering angles 0° (\circ), 1° (∇), 2° (\square), and 3° (\diamond); PES (\bullet)—vibrational population from photoelectron spectroscopy (Ref. 8). The data are normalized to have the same areas under each of the curves.

analysis for laboratory scattering angles 0° – 3° are shown in Fig. 8 as populations of vibrational levels. For comparison, the populations of H_2S^+ vibrational states as obtained by photoelectron spectroscopy⁸ are given, also. The charge transfer data in Fig. 8 show that the population of vibrational levels are very similar to those from photoelectron spectroscopy at 0° and indicate a slight increase of the population of $v_1^+ > 1$ –3 with the increasing scattering angle, though the error bars on the data points are appreciable at higher scattering angles.

IV. DISCUSSION

The single-electron charge transfer between a doubly-charged ion and a neutral particle, leading to two singly-charged ions, can be described in terms of crossing of two basic potential energy terms. If one for simplicity assumes that the molecular target is a structureless, atomlike particle (of the same IP as the molecule) the process can be described as a crossing of two potential energy curves [Fig. 9(a)]: an ion-induced dipole attractive potential combined with repulsion at small internuclear separations for the reactants, and a Coulomb repulsion curve between the two products of the same charge. The transition is located in the vicinity of the crossing point R_c , and can be usually treated in terms of the Landau–Zener model. The system on the way from the reactant to the product asymptote can follow two different pathways depending on whether the transition occurs on the way in or on the way out, i.e., before or after the classical turning point was reached. The two pathways are equally probable, but because the system moves in successive parts of the trajectory under the influence of different potentials, the scattering related to the two pathways is different.¹⁴ Schematic trajectories in Fig. 9(b) illustrate this point. The

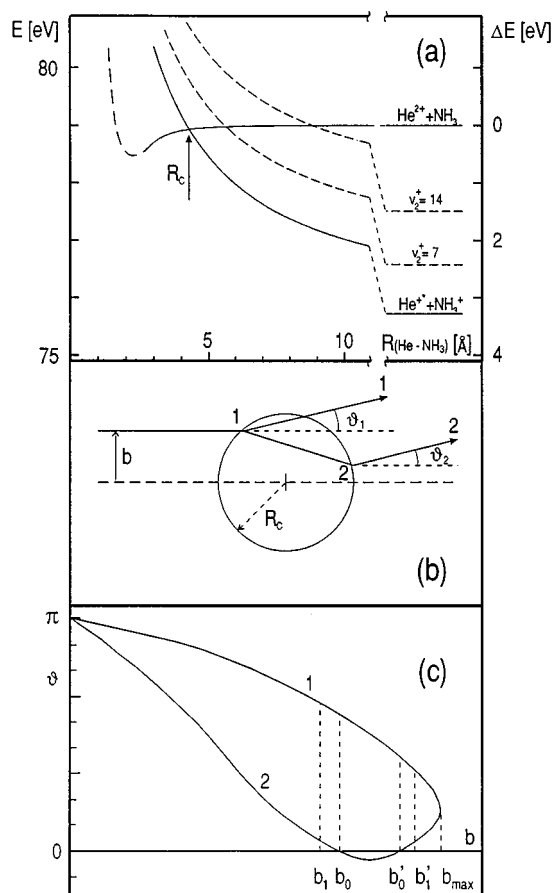


FIG. 9. (a) Potential energy curves for reaction (2) (schematically) plotted as a function of the interparticle distance $R(\text{He-NH}_3)$; R_c , crossing with the Coulomb repulsion curve $\text{He}^{2+}+\text{NH}_3^+$ ($v_2^+=0$) at 4.2 Å; dashed curves indicate schematically positions of crossings with diabatic curves of $v_2^+=7$ and $v_2^+=14$. (b) Schematic trajectories corresponding to pathways 1 and 2 (see text) for an impact parameter b ; transitions occurring at the vicinity of the crossing radius R_c at 1 or 2 lead to different scattering angles, ϑ_1 and ϑ_2 , respectively. (c) Deflection function (schematically) for the charge transfer process (1); two branches, corresponding to pathways 1 and 2 join smoothly at b_{max} , contributions to $\vartheta=0^\circ$ come from impact parameters b_0 and b_0^+ .

classical deflection function [Fig. 9(c)] then exhibits two branches related to the two pathways, with an apex at b_{max} which lies closely to or slightly above R_c (for very low collision energies) and is displaced towards positive scattering angles.¹⁴ The upper branch corresponds to the pathway 1, the lower branch, with a rainbow minimum, to pathway 2. It is clear from Fig. 9(c) that several impact parameters b may contribute to the same scattering angle. However, the Landau-Zener transition probability treatment indicates that the most significant contributions to the cross section result from large impact parameters close to b_{max} .¹⁴

In the case of collisions involving molecular systems, crossing of multidimensional potential energy surfaces and excitation of vibrational and rotational states of the molecular product must be taken into consideration. The treatment is then simplest for high-energy (keV) collisions, where the collision time is much shorter than the vibrational period of the molecular motion, $t_{\text{coll}} \ll t_{\text{vib}}$. In this case the molecule may be regarded as “frozen” during the collision, and the population of vibrational states of the molecular product may

be expected to be determined by the respective Franck-Condon factors between the neutral molecule and the molecular ion. For very slow collisions ($t_{\text{coll}} \gg t_{\text{vib}}$) models which assume well separated crossing between distinct vibrational states were applied.¹⁵

In our case the velocity of the projectile of 70 eV is 5.8×10^6 cm/s, and for the case of reaction (2) with NH₃ the average passage through the region of crossings with NH₃⁺ states $v_2^+=14$ ($R_c=9$ Å) [see dashed curves in Fig. 9(a)] and $v_2^+=0$ ($R_c=4.2$ Å) is about $t_{\text{coll}} \approx 1.5 \times 10^{-14}$ s to be compared with the vibrational periods of the NH₃ molecule $t(v_2)=3.7 \times 10^{-14}$ s (bending mode) and $t(v_1)=1 \times 10^{-14}$ s (symmetric stretch). An analogous situation holds for scattering from H₂S. Thus in our case the ratio of the times is an intermediate between the two extremes described above. In this situation another characteristic transition time t_0 becomes important defined by¹⁶

$$t_0 = \left(\frac{\hbar}{v_R |F_1 - F_2|} \right)^{1/2}. \quad (6)$$

In Eq. (6) v_R is the relative velocity, and F_1 and F_2 are the slopes of the crossing diabatic potentials. If t_0 is smaller than the vibrational period, the passage through the crossing region may be treated in a single-crossing approximation and one may expect a vibrational distribution of the molecular product not much different from the Franck-Condon distribution.¹⁶ Due to the steepness of the Coulomb repulsion curve, $t_0 \approx 1 \times 10^{-15}$ s in our case and the approximation is applicable. We may, therefore, expect a distribution of final molecular vibrational states which will show small deviations from the Franck-Condon-type distribution.

The ionization process leading to the ground state of NH₃⁺ (X^2A_1) is a result of a removal of a “nonbonding” electron from the outermost molecular orbital ($3a_1$) of the ground state molecule, NH₃ ($1a_1$)² ($2a_1$)² ($1e$)⁴ ($3a_1$)², X^1A_1 . The ionization is accompanied by a change in the geometry of the pyramidal ground state neutral molecule to the planar ground state of the ion. The geometrical change results in population of a long progression of vibrational states connected in photoionization with the pure “umbrella” bending mode v_2^+ of the ion, with spacings ranging from 111 to 140 meV.¹¹ In addition, the photoionization study¹¹ showed a weak, similarly spaced progression, underlying the aforementioned series and shifted by about 340 meV toward higher energies; this progression was originally assigned to the combination $v_1^+ + nv_2^+$ excitation,¹¹ a more recent theoretical analysis⁶ favors another assignment ($2v_4^+ + nv_2^+$).

One possible explanation of the small observed deviations in the energy spectrum from the photoionization vibrational level populations could be distortions of the NH₃ target by the approaching He²⁺ (Ref. 17). The shift of the peak of the charge transfer distribution at 0° by 1–2 levels can be ascribed to a change of the bending angle by a few degrees. A simple estimation from the calculated potential energy curves of the NH₃-NH₃⁺ system¹² indicates that a change in the bending angle from the equilibrium 22.1° to 23.9°–25° would lead to the observed shift in the position of the peak of the distribution. From the bond angle one would expect a gradual, consistent change in the population distribution with

increasing scattering angle, presumably a further slight shift of the distribution peak to higher energies. This is, however, not the case: at 1° and 2° the distribution acquires a low-energy shoulder and its overall width increases. Indeed, it appears to consist of two overlapping distributions, one—close to the photoelectron distribution—which grows in importance with increasing scattering angle, and another with a peak shifted by 1–2 quanta to higher energies which prevails at 0° and decreases in importance with increasing scattering angle.

An alternative explanation of the observed deviations in the vibrational level populations is based on two overlapping vibrational progressions: one due to the pure ν_2^+ bending progression, growing in importance with increasing scattering angle, and the other one due to a combination excitation $\nu_1^+ + n\nu_2^+$ (or $2\nu_4^+ + n\nu_2^+$), prevailing at 0° and decreasing in importance with increasing scattering angle. The latter was observed in photoionization as the weak band underlying the ν_2^+ progression.^{6,7} The combination band could conceivably be excited much more strongly in the charge transfer process due to the fact that the stretching vibration—of a higher frequency than the bending vibration—can be expected to be more strongly coupled to the translational motion of the system.

The discussion of the reasons which may account for the deviation of the population of vibrational levels of the molecular product from the Franck–Condon distribution has to be regarded as qualitative only. A detailed knowledge of the potential energy surface is needed to make a quantitative prediction possible.

The ionization of H_2S to the ground electronic state of the ion, $\text{H}_2\text{S}^+(X^2B_1)$, requires removal of an electron from the highest occupied ($1b_1$) orbital of the ground state molecule $\text{H}_2\text{S}(a_1)^2(b_2)^2(a_1)^2(b_1)^2$, X^1A_1 , causing very little change in the bond angle and bond length.¹⁸ This is consistent with the nonbonding character of the ($1b_1$) orbital which is mainly the sulphur lone-pair orbital. The Franck–Condon factors then favor mostly the transition to the vibrational ground state of the cation, as confirmed by photoelectron spectra⁸ which show only very small populations of levels $\nu_1^+ > 0$ (see Fig. 8).

In the charge transfer spectra with He^{2+} the population of the vibrational states of H_2S^+ is almost the same as the Franck–Condon population at θ_{LAB} of 0° and 1° being within the limits of accuracy of the experiment. At higher scattering angles the population of $\nu_1^+ > 0$ slightly increases, but the difference is small and $\nu_1^+ = 0$ remains, by far, the most highly populated vibrational level. This is consistent with a very small distortion of the bending angle and/or of the bond length in the target molecule by the approaching projectile, causing only a small deviation from the Franck–Condon factors. Again, only a detailed knowledge of the respective potential energy surfaces could lead to a quantitative evaluation of this effect.

V. CONCLUSIONS

Single-electron charge transfer between He^{2+} and NH_3 and H_2S was investigated at the projectile energy of 70 eV

using the translational spectroscopy method with a resolution of 120 meV. The spectra obtained at several scattering angles close to zero show that the products are $\text{He}^{+*}(^2P)$ and the molecular ion in its ground state.

From the high-resolution spectra populations of the vibrational states of the molecular ion could be derived; the vibrational state distributions differ only slightly from the distributions obtained by photoelectron spectroscopy and the changes may be regarded as being due to interaction of the molecular target with the approaching projectile.

In the case of NH_3 either a small change in the bending angle by about 2° – 3° may account for the difference or, alternately, a change in the relative intensities of the pure bending mode progression ν_2^+ and of the combination mode progression $\nu_1^+ + n\nu_2^+$ ($2\nu_4^+ + n\nu_2^+$).

In the case of H_2S , the $\nu_1^+ = 0$ level is populated with highest probability both in photoelectron and charge transfer spectra; a small increase in the population of $\nu_1^+ > 0$ in the charge transfer spectra is presumably due to a very small distortion of the molecular target by the ion projectile.

ACKNOWLEDGMENTS

Two of the authors (M.F. and T.R.) express thanks for the financial support of the Max Planck Gesellschaft of this research, one of them (Z.H.) gratefully acknowledges the Alexander von Humboldt Award Fellowship and the hospitality of the Max-Planck Institut für Strömungsforschung during his visits. Parts of the work were supported by Grant No. 203/93/0246 of the Grant Agency of the Czech Republic and Grant No. 440410 of the Grant Agency of the Czech Academy of Sciences.

¹R. K. Janev and H. Winter, *Phys. Rep.* **117**, 265 (1985).

²D. Mathur, *Phys. Rep.* **225**, 193 (1993).

³C. E. Moore, *Atomic Energy Levels*, Natl. Bur. Standards, Circ. No. 467 (US GPO, Washington, 1971).

⁴A. A. Radzig and B. M. Smirnov, *Reference Data on Atoms, Molecules, and Ions* (Springer, Berlin, 1985).

⁵M. Fárník, Z. Herman, T. Ruhaltinger, J. P. Toennies, and R. G. Wang, *Chem. Phys. Lett.* **206**, 376 (1993).

⁶P. Botschwina, in *Ion and Cluster Ion Spectroscopy and Structure*, edited by J. P. Maier (Elsevier, Amsterdam, 1989).

⁷G. Reiser, W. Habenicht, and K. Müller-Dethlefs, *J. Chem. Phys.* **98**, 8462 (1993).

⁸L. Karlsson, L. Mattsson, R. Jadrny, T. Bergmark, and K. Siegbahn, *Phys. Scr.* **13**, 229 (1976).

⁹W. Maring, J. P. Toennies, R. G. Wang, and H. B. Levene, *Chem. Phys. Lett.* **184**, 262 (1991); *J. Chem. Phys.* (to be published).

¹⁰T. M. Austin, J. M. Mullen, and T. L. Bailey, *Chem. Phys.* **10**, 117 (1975).

¹¹J. W. Rabalais, L. Karlsson, L. O. Werme, T. Bergmark, and K. Siegbahn, *J. Chem. Phys.* **58**, 3370 (1973).

¹²H. Ågren, I. Reineck, H. Veenhuisen, R. Maripuu, R. Arneberg, and L. Karlsson, *Mol. Phys.* **45**, 477 (1982).

¹³I. Fisher, A. Lochschmidt, A. Strobel, G. Niedner-Schatteburg, K. Müller-Dethlefs, and V. Bondybey, *J. Chem. Phys.* **98**, 3592 (1993).

¹⁴B. Friedrich, Š. Pick, L. Hládek, Z. Herman, E. E. Nikitin, A. I. Reznikov, and S. Ya. Umanskii, *J. Chem. Phys.* **84**, 807 (1986).

¹⁵E. Bauer, E. R. Fisher, and F. R. Gilmore, *J. Chem. Phys.* **51**, 4173 (1969).

¹⁶M. S. Child, *Molecular Collision Theory* (Academic, New York, 1974).

¹⁷M. Lipeles, *J. Chem. Phys.* **51**, 1252 (1969).

¹⁸R. N. Dixon, G. Duxbury, M. Horani, and J. Rostas, *Mol. Phys.* **22**, 977 (1971).